RSC Advances

ROYAL SOCIETY OF CHEMISTRY

www.rsc.org/advances

Conductivity stability and its relationship with filler network structure of Elastomer Composites with Combined Fibrous/Layered Nickel-Coated Fillers

Nanying Ning [1,2], Suting Liu [2],Qian Shao [2], Shani Yan [2], Hua Zou [2],

Liqun Zhang [1,2] , and Ming Tian [1,2*]

1. State Key Laboratory of Organic-Inorganic Composites, Beijing University of Chemical Technology, Beijing 100029, China;
2. Key Laboratory of Carbon Fiber and Functional Polymers, Ministry of Education, Beijing University of Chemical Technology, Beijing 100029, China.

Abstract: Nickel-coated graphite (NCG) with layered structure and nickel-coated carbon fiber (NCF) with fibrous structure were simultaneously introduced into silicone matrix to prepare conductive elastomer composites (CEC) with high electrical conductivity and high conductivity stability. The effect of the volume fraction of fillers, the volume ratio of NCF/NCG, external strain and relaxation time on the conductivity and conductivity stability of the composites were studied. The results showed that the percolation threshold decreased with the increase in volume ratio of NCF/NCG. The conductivity and conductivity stability increased with the increase in the volume fraction of fillers, the volume ratio of NCF/NCG and the relaxation time, but decreased with the increase in external strain. The two dimensional morphology

---

[*] **Corresponding author.** College of Materials Science and Engineering, Beijing University of Chemical Technology, No. 15 Bei-San-Huan East Road, ChaoYang District, Beijing, 100029, China. Tel.: +86 10 6443 4860; Fax: +86 10 6443 3964. E-mail: tianm@mail.buct.edu.cn (Ming Tian)

of conductive filler network was characterized by using environmental scanning electron microscopy and the three dimensional network was characterized by using rubber processing analysis. The relationship between conductive filler network and conductivity/conductivity stability is established for the first time to provide guidance for the preparation of high performance CEC.

Keywords: A. conductive elastomer composites; B. conductivity C. conductivity stability; D. conductive filler network

1. Introduction

Conductive elastomer composites (CEC) have been widely used in industry such as electromagnetic interference (EMI) shielding, electrostatic charge dissipation, touch control switches, sensor and surface heaters by virtue of the good flexibility, elasticity and sealability of elastomers, and the good electrical conductivity of conductive fillers [1-3]. The most commonly used conductive fillers include metal powders, metal-coated inorganic particles and electrically conductive carbon fillers (such as carbon black (CB), carbon fiber, carbon nanotubes (CNTs) and graphene) [4-9]. CB has the advantage of low density, low cost and high environmental stability, but CB has low electric conductivity, thus are mainly used as antistatic material. The commonly used metal powders such as silver (Ag) and copper (Cu), have very high electric conductivity, but they are quite expensive and have high densities. Comparing with metal powders, metal-coated inorganic particles such as silver coated-glass beads, silver coated-aluminum, and nickel-coated graphite etc, combine the high electrical conductivity, low density and low cost, thus are widely used as EMI shielding materials in the areas of aerospace, precision instrument, and communication base station [10-12]. Of these metal-coated fillers, nickel-coated fillers exhibit better oxidation resistance and cheaper than silver-coated fillers [13]. In addition, the newly developed conductive nanofillers such as CNTs and graphene are far from industrial application.

To achieve high conductivity, the formation of conductive path is a key, as demonstrated by the conductive theories, such as the percolation theory, tunnel effect theory and electric field emission theory [14-16]. The formation of conductive path is mainly affected by the volume fraction and shape of conductive fillers and the dispersion of fillers in matrix. The increase in the volume fraction of conductive fillers is a simple and efficient method for the formation of conductive path. However, the increase in the volume fraction of fillers can inevitably lead to the loss in flexibility and elasticity, the deteriorating in processing properties, and the increase in cost of the composites [17, 18]. Therefore, conductive fillers with different shapes were usually introduced simultaniously to achieve a high conductivity at low filler volume fraction [19-21]. For example, silver-coated glass beads combined with silver-coated carbon fibers were used as conductive fillers in silicone rubber. The as-prepared composites had a much higher conductivity, a lower cost and better mechanical properties than that with silver-coated glass beads at the same filler volume fraction.

Theoretically, conductive path is formed by the formation of three dimensional (3D) conductive filler network [22-24]. The commonly used technique such as Scanning Electron Microscope (SEM) and Transmission Electron Microscopy (TEM) can only be used to characterize the two dimensional (2D) morphology of conductive filler network [25, 26]. In recent years, it has been reported that three dimensional (3D) conductive filler network can be characterized by using focused ion beam (FIB) SEM and 3D-TEM, but both of them are very complicated and time-consuming, and they cannot be used to characterize the 3D network of fillers with large lengths or diameters (> 50 micrometer) because of the limited scanning scope [27, 28]. Up to now, the characterization of 3D filler network, and the build-up of relationship between conductive filler network and conductivity is still a challenge.

CEC are subjected to tensile stress or compress stress during storage, installation and application, and will inevitably destroy the conductive network, and thus affect the electrical conductivity of the composites. It has been reported that the tensile/compression strain and the strain rate has a significant effect on the conductivity stability of CB/rubber composites [29]. In addition, the effects of storage time, aging time, tensile strain, stretching time, and salt spraying on the conductive stability of NCG/silicone rubber composites were systematically studied [30]. Despite of these studies on conductivity stability of CEC, the relationship between filler network and the conductivity stability of CEC has not been reported yet.

Of various elastomers, silicone elastomer has good flexibility, high elasticity, high strain recovery ability, good thermal stability, excellent resistance to high and low temperatures, low viscosity, and low hardness, and thus it is widely used as CEC material. Herein, nickel-coated graphite (NCG) with layered structure and nickel-coated carbon fiber (NCF) with fibrous structure were simultaneously introduced into silicone matrix to prepare CEC with high electrical conductivity, high conductivity stability, high elasticity and low-cost. Comparing with NCG, NCF with a larger aspect ratio could form a conductive network more easily, thus could increase the electrical conductivity and conductivity stability at the same volume fraction of fillers. However, NCF is much more expensive than that of NCG. In addition, the addition of high volume fraction of NCF can deteriorate the processing properties. Therefore, NCG was used to decrease the cost and improve the processing properties of the composites. The effect of volume ratio of NCF/NCG, external strain and relaxation time on the conductivity and conductivity stability of the composites are systematically studied. The 2D morphology of conductive filler network was characterized by using environmental scanning electron microscopy (ESEM) and the 3D conductive network was characterized by using rubber processing analysis (RPA). The relationship between conductive filler network structure and conductivity/conductivity stability was studied to provide guidance for the preparation of CEC with high conductivity and high conductive stability.

2. Experimental

2.1. Materials

Polymethylvinylsiloxane (PMVS, Grade 110-2, 1.05 g/cm^3, M_n=5.7×10^5 g/mol) was supplied by Beijing Huaer Co., Ltd. (China). The molecular structure of PMVS was shown in Scheme 1. The glass transition temperature of PMVS determined by

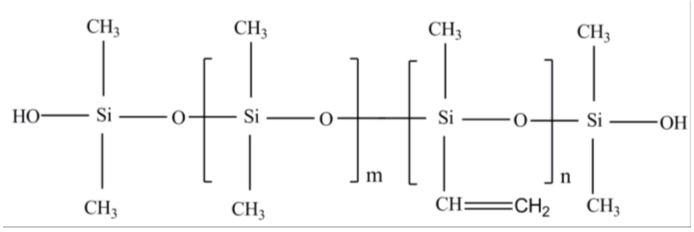

Scheme 1: Molecular structure of PMVS

Differential Scanning Calorimetry (DSC) was -123 °C. The vinyltriacetoxy silane **(**coupling agent, A151, $C_8H_{12}O_6Si$) was supplied by Beijing Reagent Chemical Corporation (China). The vulcanizing agent (2,5-dimethyl-2,5-bis(tert-butyl peroxy) hexane, DBPMH) was supplied by Qiangsheng Chemical Co., Ltd., China. NCG (Grade E-FILL2701) with 60wt% of Nickel and NCF (Grade E-FILL2901) with 67wt% of Nickel were supplied by Sulzer Metco (Canada) Inc. The lateral size of NCG is 30-300 μm, whereas the thickness of NCG is 35-40 μm. The length of NCF is 50-750 μm, whereas the diameter of NCF is 7-10 μm. Thus, the aspect ratio of NCF (5-100) is much larger than that of NCG (1-9).

2.2. Preparation of composites

First, we mixed NCF/NCG conductive fillers (the volume ratio of NCF/NCG varies from 10/0, 7/3, 5/5, 3/7 to 0/10) by using homogenizer for 3-5 minutes, and then we added the coupling agent (3wt% of the weight of conductive fillers) into the mixture of conductive fillers. Then, various compositions of PMVS, the mixture of conductive fillers (the total volume fractions of conductive fillers range from 1 to 32 vol.%), and the vulcanizing agent (2wt% of the weight of PMVS) were sequentially added into a Haake torque rheometer (Typ557-1302, Thermo Haake Co., Ltd., Germany) to prepare NCF/NCG/PMVS composites at a temperature of 90 °C, rotor speed of 20 rpm and mixing time of 10 min. The composites was vulcanized on a platen press at 170 °C under 10 MPa for 20 min and then vulcanized in a draught drying cabinet under air atmosphere at 200 °C for 2 h. The coupling agent was used to increase the interfacial interaction between the fillers and the polymer matrix, as schematically represented in Scheme 2.

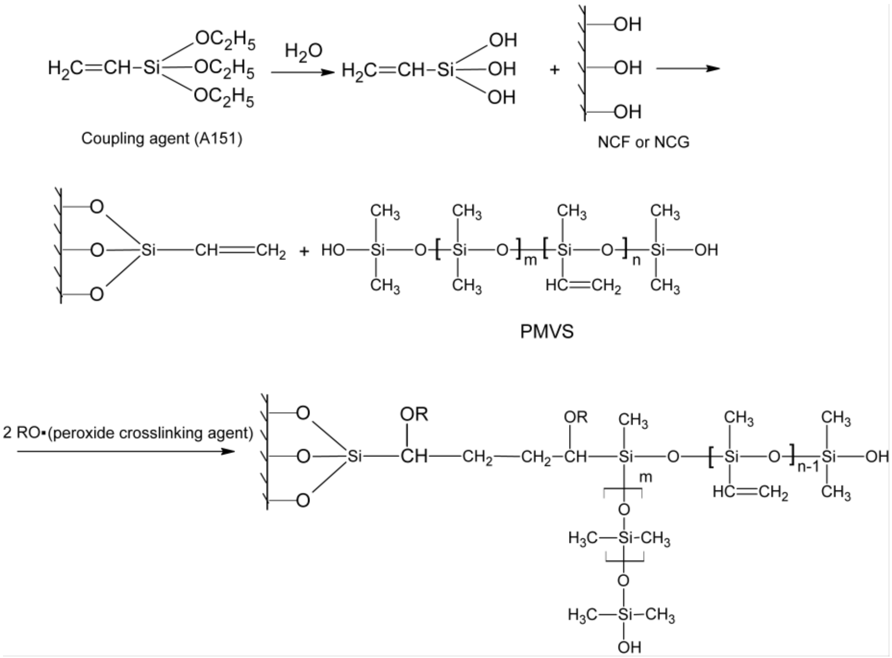

Scheme 2: Schematic representation of the effect of the coupling agent on increasing the interfacial interaction between the fillers and the elastomer matrix

The cured sheets were then cut into samples with the width, length, and thickness of 10 mm, 100 mm, and 1 mm, respectively. The samples were kept at the standard experimental conditions (temperature of 23±2°C, relative humidity of 50±10%) for 24 h before testing.

2.3. Characterizations

The electrical resistance of composites with a high resistivity ($\geq 10^4\ \Omega$) was measured by using a high resistance meter (PC68, Shanghai Precision & Scientific Instrument Co., Ltd., China). A DC Bridge (QJ84, Shanghai Zhengyang Instrument Factory, China) was used to measure the volume conductivity of composites with low resistivity according to Chinese standard GB/T 2439-2001. The volume resistivity ρ was calculated by:

$$\rho = R \cdot S/L$$

where R is the electrical resistance of the sample, S is the cross-sectional area, and L is the length of the sample. Five samples were tested for each composite and the average value was reported.

The conductive stability was characterized by the ratio of volume resistivity measured before tension to that measured after tension. The samples were stretched to a certain strain (5%, 10%, 15%, or 20%) by using a self-made tensile installation and kept for 10 min. [21] The volume resistance was measured after the sample was placed in the standard experimental conditions for 5-30 min for recovery. All these elastomer composites can almost recover to their initial shapes after 30 min recovery time.

The morphology of the composites was observed by using ESEM (XL-30, Philips-FEI Company, Eindhoven, USA) with an acceleration voltage of 15 V. The samples were first cryogenically fractured in liquid nitrogen and coated with gold with a thickness of 10-20nm. The network structure of conductive fillers in the composites was characterized by using a Rubber Process Analyzer (RPA, Alpha Technologies Co., USA) at 60 ^{o}C and a frequency of 1 Hz in the strain amplitude range of 0.28% to 400%.

3. Results and discussion

3.1 Conductivity

The volume resistivity of conductive composites decreases with the increase in the volume fraction of conductive fillers. Especially, the volume resistivity decreases sharply as the volume fraction of conductive fillers in a composite reaches a critical value because of the formation of conductive network in the matrix [31]. In this case, the composite becomes electrical conductor. The percolation threshold is defined as the critical value of the volume faction of fillers (V_f) at which the greatest change of volume resistivity occurs, corresponding to the greatest slop of the percolation curves. Thus, d (log ρ) / dV_f was calculated, and the results are shown in the inset of Fig. 1.

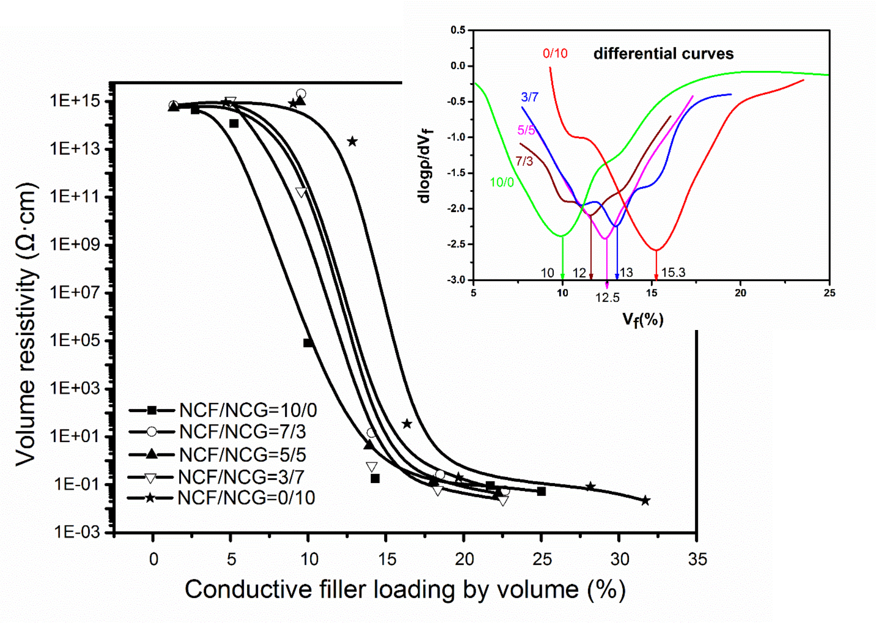

Fig. 1. Plots of volume resistivity versus volume fraction of filler for various composites. The inset shows plots of d (log ρ) versus dV_f.

Fig. 1 shows the percolation curves representing the relationship between volume resistivity of the composite and the volume fraction of conductive fillers. The volume resistivity of all the composites decreases by 14 orders of magnitude as the volume fraction of conductive fillers reaches the percolation threshold. The corresponding differential curves obtained from the percolation curves are shown in the inset of Fig. 1. The percolation thresholds (the lowest points of the differential curves) of all the composites can be clearly seen. Obviously, the percolation threshold of pure NCG/PMVS composite is the largest (15.3 vol.%) because of the layered structure of NCG. The percolation threshold decreases with the increase in the ratio of NCF/NCG, and it decreases to 10 vol.% for pure NCF/PMVS composite. In addition, the conductivity of the composites increases with the increase in the ratio of NCF/NCG at the same volume fraction of fillers. These results suggest that it is much easier for NCF with fibrous structure to form a conductive network in the composites than that for NCG with layered structure due to its lower aspect ratio than that of NCF, consistent well with previous studies. The preparation of CEC with high conductivity at lower volume fraction of filler facilities the achievement of CEC with high elasticity and good flexibility, as will be discussed later.

3.2 Conductive stability

The electric conductivity of CEC is inevitably influenced by some external forces such as stretching and compression during the storage, installation and application of these materials. The conductivity stability is thus very important for the achievement of a long lifetime of these materials. Therefore, the effect of the volume fraction of conductive fillers, the volume ratio of fibrous to layered fillers as well as the external strain and recovery time on the conductive stability of the composite is systematically studied. The change in volume resistivity is represented in terms of relative resistivity (ρ/ρ_0), where ρ_0 and ρ refers to the resistivity of the as-prepared samples and the samples after exerting a certain strain.

3.2.1 Effect of total volume fraction of conductive fillers

In order to study the effect of total volume fraction of conductive fillers on the conductivity stability of the composites, the variation of relative resistivity (ρ/ρ_0) with the volume ratio of NCF/NCG at different total volume fractions of conductive fillers was studied, and the results are shown in Fig. 2. Φ_{NCF} and Φ_{NCF} represent volume fraction of NFC and NCG, respectively. Based on the percolation threshold (15.3 vol.%) of pure NCG/PMVS composites, three kinds of total volume fraction of conductive fillers were used: near or even lower than the percolation threshold of the composites (14 vol.%), slightly higher than the percolation threshold (18 vol.%), and much higher than the percolation threshold (22 vol.%). All the composites were subjected to the same tensile strain of 10% for 10 mins and then relaxed for 30 mins. ρ/ρ_0 of NCG/PMVS composites cannot be obtained at the volume fraction (14 vol. %) lower than the percolation threshold (15.3 vol. %). At the same volume ratio of NCF/NCG, ρ/ρ_0 is obviously decreased with the increase in the total volume fraction of conductive fillers from 14% to 22%, indicating the increase in conductivity stability of the composites with the increase in the total volume fraction of fillers. This is ascribed to the formation of more stable conductive network with the increase in the total volume fraction of conductive fillers, as will be discussed in section 3.3. Thus, one of the most effective ways to improve the conductivity and conductivity stability of the CEC is to increase the total volume fraction of the conductive fillers. However, the increase in the volume fraction of fillers can result in the low flexibility, and high cost [13, 33]. In addition, the increase in the volume fraction of fillers can lead to the increase in viscosity because the viscosity of elastomer, the degree of crosslinking, and the interfacial adhesion between elastomer and NCF or the interfacial adhesion between elastomer and NCG were the same for each composite.

On the other hand, for the composites with the same total volume fraction of conductive fillers, the relative resistivity decreases with the increase in the volume ratio of NCF/NCG, indicating the increase in conductivity stability of the composites with larger volume ratio of NCF/NCG.

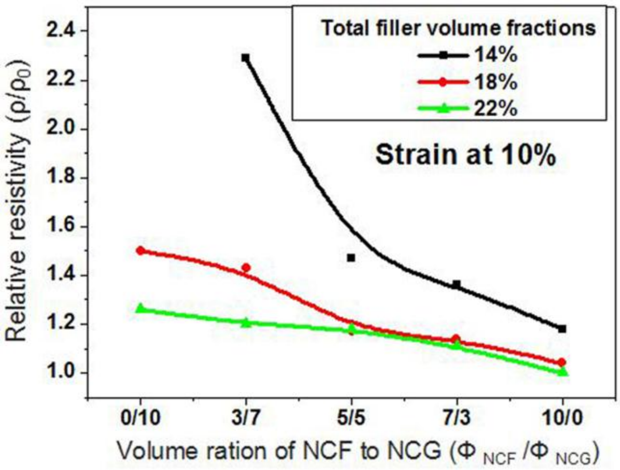

Fig. 2. Plots of relative resistivity (ρ/ρ0) against volume ratio of NCF/NCG for NCF/NCG/PMVS composites with different total volume fractions of filler

3.2.2 Effect of tensile strain

The variation of ρ/ρ_0 against tensile strain after stretching for 10 min and then relaxing for 30 min for the composites with different volume ratios of NCF/NCG is shown in Fig. 3. The total volume fraction of conductive fillers is 18 vol%, higher than the percolation threshold (10-15.3 vol. %) of all the composites filled with the nickel-coated fillers. We can observe that ρ/ρ_0 increases with the increase in tensile strain from 5%-20 % for the composites with the same volume ratio of NCF/NCG, suggesting the decreased conductivity stability of the composites with the increase in external tensile strain, consistent well with previous study [32]. The reason is that the space between the conductive fillers increases with the increase in the strain, leading to the more severe disruption of the conductive network with the increase in external tensile strain, as will be discussed later. Meanwhile, the relative resistivity decreases with the increase in volume ratio of NCF/NCG at the same tensile strain, again suggesting the increased conductivity stability of the composites with the increase in the volume ratio of fibrous conductive fillers (NCF).

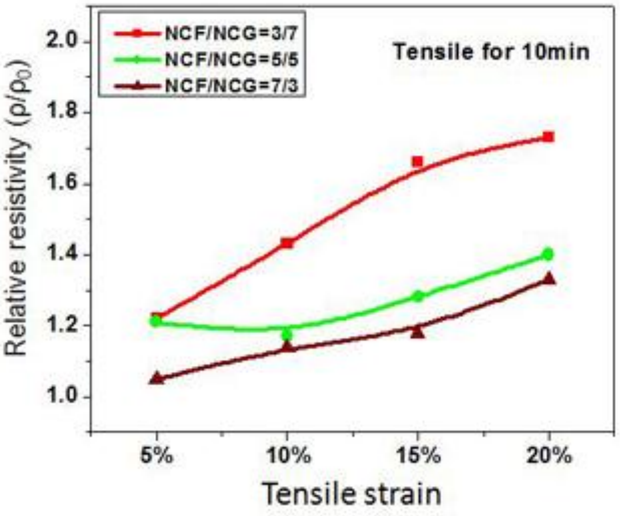

Fig. 3. Plots of relative resistivity (ρ/ρ0) against tensile strain for NCF/NCG/PMVS composites with different volume ratios of NCF/NCG (Vf=18%)

3.2.3 Effect of recovery time

The conductive filler network of the composites can be disrupted under certain tensile strain. However, the filler network can be gradually recoverd with the increase in recovery time. Thus, the relaxation time has an obvious effect on the conductivity stability of the composites. To study the effect of recovery time on the conductivity stability of the composites, the variation of ρ/ρ_0 against recovery time of the composites with different volume ratios of NCF/NCG at different strains was studied, and the results are shown in Fig. 4. We can observe that the ρ/ρ_0 of the composite before recovery at the low volume ratio of NCF/NCG (0/10 and 3/7) after subjected to tensile strain of 5%-20% for 10 minutes is very large, as shown in Fig. 4 (a) and Fig. 4 (b). This is ascirbed to the severe disruption of conductive network caused by the largely increased space between conductive fillers after exerting a tensile strain as the volume fraction (18 vol.%) of conductive fillers approaching the percolation threshold (15.3 vol.%). At the same volume ratio of NCF/NCG, the ρ/ρ_0 of the composite before recovery is significantly decreased with the decrease in tensile strain. At the same tensile strain, the ρ/ρ_0 of the composite before recovery is significantly decreased with the increase in the volume ratio of NCF/NCG. At the same tensile strain, the ρ/ρ_0 of all the composites decreases rapidly with the increase in recovery time during the first 5 mins of relaxation, suggesting the gradual recovery of disrupted conductive filler network under tensile strain with the increase in recovery time. Then, the relative resisitivity of each composite keeps almost constant with the further increase in relaxation time (> 5min) at the same strain. The reason is that a certain relaxation time is required for the rubber molecular chains to reach a steady state after subjected to a certain strain, indepedent of the kind and the total volume fraction of fillers [30]. The recovery of conductivity at a short relaxtion time (5 mins) is ascribed to the very good flexibility of silicone elastomer macromolecules. The true values of ρ/ρ_0 are that tested under the relaxation time of 5-30 min, which are plotted in the inset of Fig. 4. We can observe that the ρ/ρ_0 of each composite increases with the increase in the strain, again indicating the decreased conductivity stability by exerting a higher tensile strain. Meanwhile, the ρ/ρ_0 decreases with the increase in volume ratio of NCF/NCG at the same strain, and it even decreases to 1.1, again indicating the increased conductivity stability by using fibrous filler (NCF).

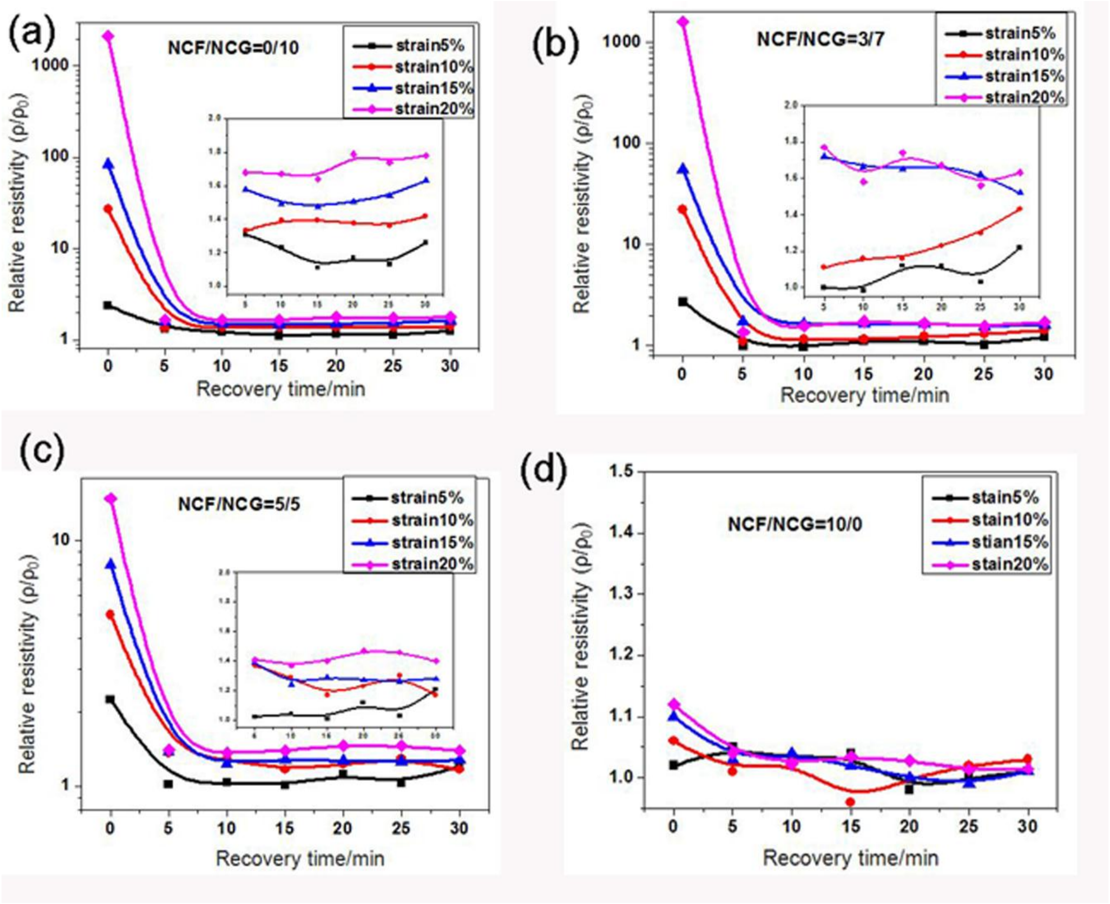

Fig. 4. Plots of relative resistivity (ρ/ρ0) against recovery time for NCF/NCG/PMVS composites with different volume ratios of NCF/NCG (a) 0/10, (b) 3/7, (c) 5/5, (d) 10/0 at different tensile strains (Vf=18%)

3.3 The relationship between conductivity stability and conductive filler network

The conductivity and conductivity stability of the conductive rubber composite is dominated by the conductive filler networks. The 2D morphology of conductive filler network of the composites with different total volume fractions of conductive fillers (NCF and NCG) at a fixed volume ratio of NCF/NCG (5/5) was characterized by using ESEM, and the results are shown in Fig. 5. NCF or NCG are almost isolated with one another and no conductive filler network is formed as the volume fraction (9 vol. %) of fillers lower than the percolation threshold (12.5 vol.%), as shown in Fig. 5

(a). NCF or NCG are connected with one another with the increase in the volume fraction of total fillers to 14 vol. % (see Fig. 5 (b)), suggesting the formation of conductive network. NCF or NCG are closely connected with one another with the further increase in the volume fraction of total fillers to 22 vol. % (see Fig. 5 (c)), leading to the formation of a stronger conductive filler network. Thus, a stronger conductive filler network formed by the increase in volume fraction of total fillers leads to the increase in the conductivity and conductivity stability of the composites, as demonstrated in section 3.1 and 3.2.

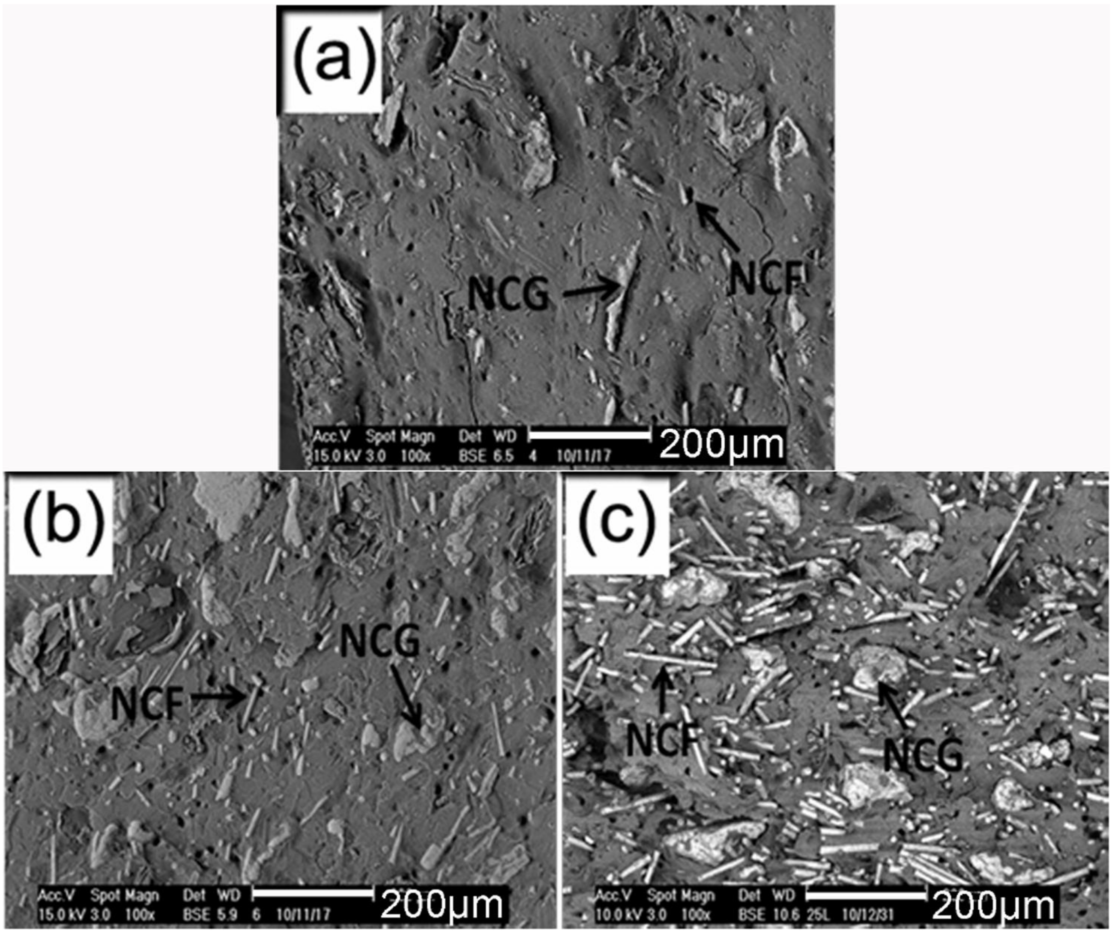

Fig. 5. ESEM micrographs of the composites with different volume fractions of conductive filler (NCF/NCG=5/5): (a) 9%, (b) 14% and (c) 22%.

The 2D morphology of filler network of the composites with different volume ratios of NCF/NCG at a fixed volume fraction of conductive fillers (18 vol. %) was also obtained by using ESEM, and the results are shown in Fig. 6. The volume fraction of conductive fillers (18 vol. %) of all the composites is larger than the percolation threshold (10~15.3 vol. %), suggesting that conductive network structure is formed in all these composites. However, the filler network structures are obviously different for these composites with different volume ratios of NCF/NCG. The space between fillers is small for the composite with pure NCG, suggesting that NCG are connected with one another and formed a conductive filler network in the composite, as shown in Fig. 6 (a). As NCG was partially substituted by NCF, the conductive fillers have more chances to connect with one another because of the high length to diameter ratio of NCF. As a result, the space between fillers becomes smaller with the increase in the volume ratio of NCF/NCG, suggesting that a stronger conductive filler network are formed in the composite, as shown in Fig. 6 (b)-(d). The space between fillers is the smallest for the composite with the presence of only NCF, suggesting the strongest conductive filler network in the composite with pure NCF. Thus, a stronger conductive filler network formed by the increase in volume fraction of NCF also results in the increase in the conductivity and conductivity stability of the composites, as demonstrated in section 3.1 and 3.2.

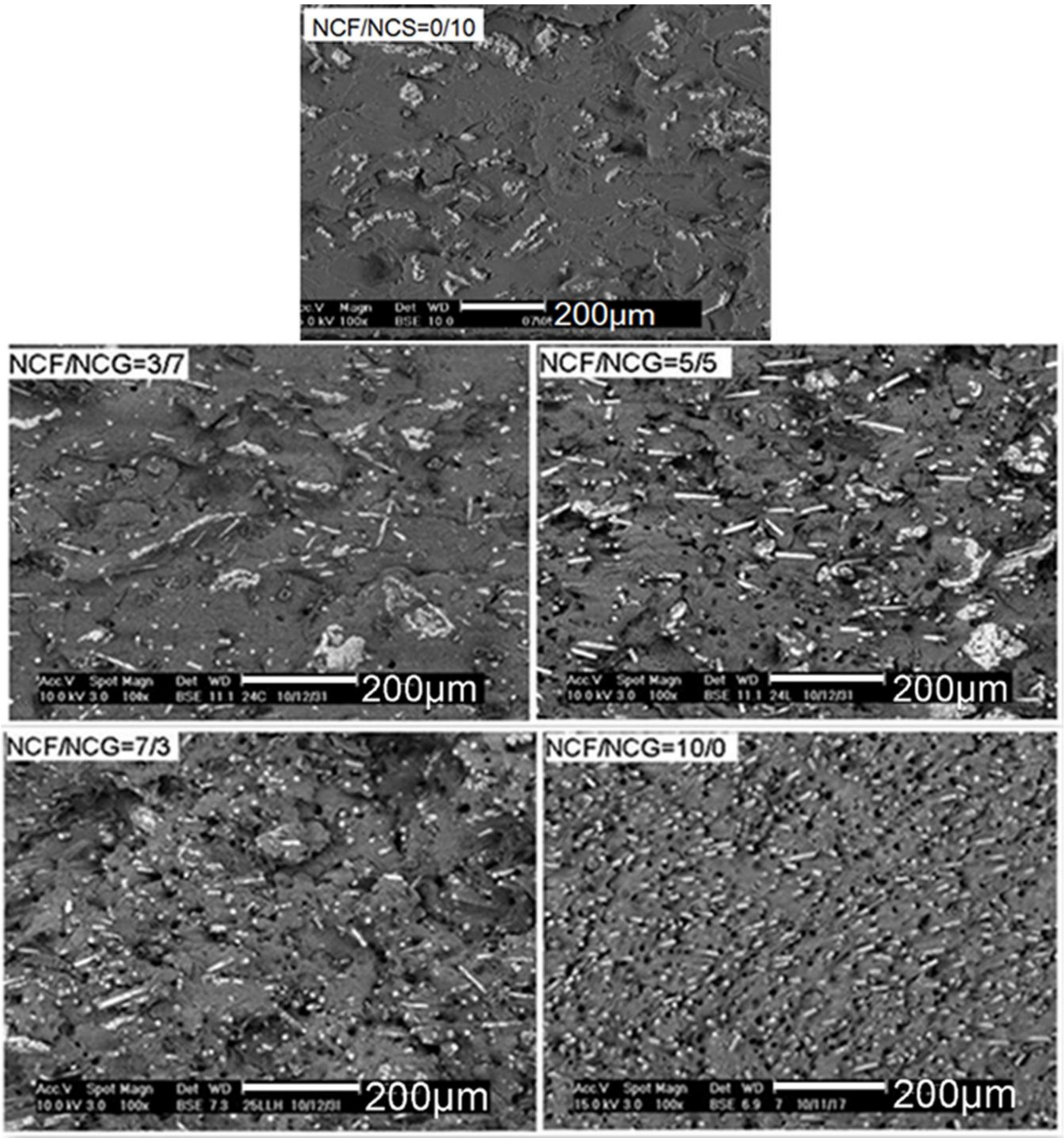

Fig. 6. ESEM micrographs of the composites with different volume ratios of NCF/NCG at constant total volume fraction of filler (18 vol%)

The 3D conductive filler network in a rubber matrix was characterized by using RPA, and the results are shown in Fig. 7 and Fig. 8. As an example, the storage modulus (G’) of the composites at a fixed volume ratio of 5/5 is shown in Fig. 7. The storage modulus (G’) decreases rapidly with the increase in shear strain for all the samples, known as Payne effect, as previously reported [34, 35]. The difference between the maximum and minimum of G', named as the modulus attenuation (△G’), was calculated according to RPA curves to reflect the strength of the 3D filler network in a rubber matrix more clearly, as shown in Fig. 8 (a). The conductivity against volume fraction of fillers is shown in Fig. 8 (b) to clearly indicate the relationship between conductivity/conductivity stability and 3D filler network. A larger △G’ indicates a stronger 3D filler network [36, 37]. As expected, △G’ is very low for all the composites with 9 vol. % of fillers at different volume ratios of NCF/NCG, indicating that 3D filler network is not formed in the composites with 9 vol. % of fillers because of the large space between conductive fillers, as demonstrated by ESEM results. As a result, the conductivity of these composites with 9 vol. % of fillers is less than 10^{-15} S/cm, as shown in Fig. 8 (b). △G’ increases with the volume fraction of fillers increasing to the percolation threshold, indicating that the 3D filler network is formed in the composites. In this case, the conductive path is gradually formed, leading to the sharp increase in conductivity. However, in this case, the conductivity stability of the composites is still low because the space between fillers is at the critical value for the formation of conductive network, which is easy to be disrupted under external stress. △G’ is further increased as the volume fraction of fillers increasing to much larger than the percolation threshold, indicating that the 3D filler network becomes stronger in the composites. In this case, the conductivity is only slightly increased or unchanged because the space between fillers is too small and is almost unchanged with the further increase in the volume fraction of fillers. However, the conductivity stability is obviously increased because of the formation of a more completed conductive path.

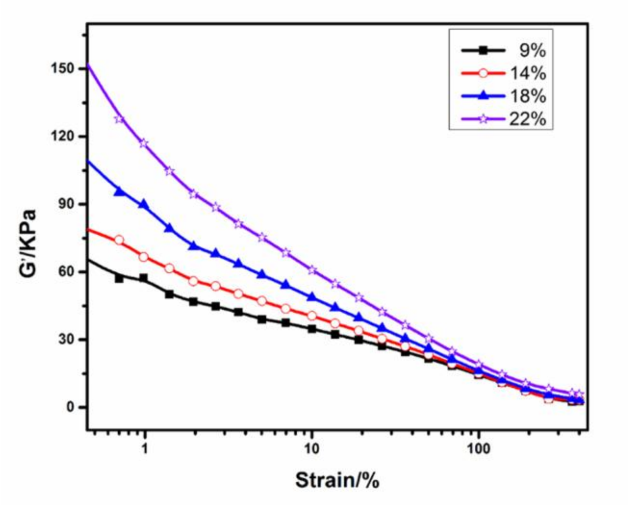

Fig. 7. Storage modulus as a function of strain for NCF/NCG/PMVS composites with different total filler volume fractions (NCF/NCG=5/5).

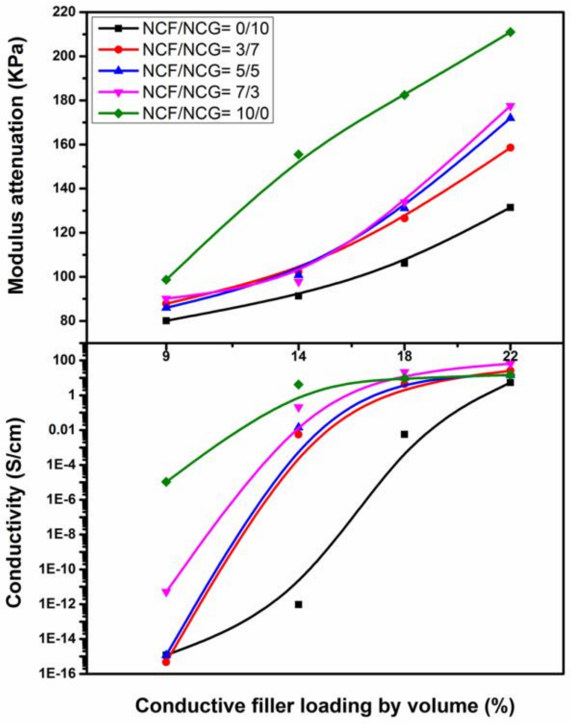

Fig. 8. Plots of (a) modulus attenuation (△G') against volume fraction of fillers, and (b) conductivity against volume fraction of fillers for NCF/NCG/PMVS composites with different total volume fractions of fillers

In addition, at the same total volume of fillers, △G' increases with the increase in volume fraction of NCF, indicating that the filler network becomes stronger with the increase in volume fraction of NCF, consistent well with the ESEM results. Correspondingly, the conductive path is much easier to be formed with the increase in volume ratio of NCF because of the formation of stronger conductive filler network, leading to the increase in both the conductivity and conductivity stability.

4. Conclusions

CEC with high electrical conductivity and high conductivity stability have been prepared by using the combined fibrous/layered nickel-coated fillers. The conductive percolation threshold of the composites is decreased with the increase in the volume ratio of NCF/NCG. The 2D morphology of conductive filler network was characterized by using environmental scanning electron microscopy and the 3D network was characterized by using rubber processing analysis. The relationship between the filler network structure and the conductivity/conductivity stability of CEC composites are established for the first time. A stronger conductive filler network structure is obtained with the increase in the volume fraction of fillers and the volume ratio of NCF/NCG, leading to the easier formation of conductive path, and thus the increase in conductivity and conductivity stability. The conductive filler network structure is disrupted under external strain, leading to the disruption of conductive path, and thus the decrease in conductivity and conductivity stability. However, the disrupted conductive filler network can be gradually recovered under certain relaxation time, resulting in the increase in conductivity and conductivity stability. This study provides guidance for the preparation of high performance CEC materials.

Acknowledgements

We would like to express our sincere thanks to the National Natural Science

Foundation of China (Grant No. 51221002) for financial supports.

References

1. A. Fletcher and M. C. Gupta, *J. Com. Mater.*, 2014, **48**, 1261.
2. H. Stoyanov, M. Kollosche, S. Risse, R. Waché and G. Kofod, Adv. Mater., 2013, 25, 578.
3. C. L. Choong, M. B. Shim, B. S. Lee, S. Jeon, D. S. Ko, T. H. Kang and U. I. Chung, *Adv. Mater*., 2014, **26**, 3451.
4. C. Morari, I. Balan, J. Pintea, E. Chitanu and I. Iordache, *Progress In Electromagnetics Research M*, 2011, **21**, 93.
5. H. Stoyanov, M. Kollosche, S. Risse, R. Waché and G. Kofod, 2013, *Adv. Mater.*, **25**, 578.
6. E. Bilotti, R. Zhang, H. Deng, M. Baxendale and T. Peijs, *J. Mater. Chem.*, 2010, **20**, 9449.
7. S. Pavlovsky and A. Siegmann, *J. Appl. Polym. Sci.*, 2009, **113**, 3322.
8. L. Lin, H. Deng, X. Gao, S. Zhang, E. Bilotti, T. Peijs and Q. Fu, *Polym. Int.*, 2013, **62**, 134.
9. H. Kim, Y. Miura and C. W. Macosko, *Chem. Mater.*, 2010, **22**, 3441.
10. A. Fletcher, M. C. Gupta, K. L. Dudley and E. Vedeler, *Compos. Sci. Technol.*, 2010, **70**, 953.
11. Z. Liu, G. Bai, Y. Huang, Y. Ma, F. Du, F. Li, T. Guo and Y. Chen, *Carbon*, 2007, **45**, 821.
12. S. Kwon, R. Ma, U. Kim, H. R. Choi and S. Baik, *Carbon*, 2014, **68**, 118.

13. H. Zou, L. Zhang, M. Tian, S. Wu and S. Zhao, *J. Appl. Polym. Sci.*, 2010, **115**, 2710.

14. P. Zhang, Y. Bin, R. Zhang and M. Matsuo, *Polymer*, 2014, **55**, 2597.

15. S. Xu, O. Rezvanian, K. Peters and M. A. Zikry, *Nanotechnology*, 2013, **24**, 155706.

16. L. Wang and L. Cheng, *Carbon*, 2014, **71**, 319.

17. S. Araby, L. Zhang, H. C. Kuan, J. B. Dai, P. Majewski and J. Ma, *Polymer*, 2013, **54**, 3663.

18. W. Xing, M. Tang, J. Wu, G. Huang, H. Li, Z. Lei and H. Li, *Compos. Sci. Tech.*, 2014, **99**, 67.

19. M. Li, C. Gao, H. Hu and Z. Zhao, *Carbon*, 2013, **65**, 371.

20. X. Qi, D. Yan, Z. Jiang, Y. Cao, Z. Yu, F. Yavari and N. Koratkar, *ACS Appl. Mater. Inter.*, 2011, **3**, 3130.

21. K. Hilarius, D. Lellinger, I. Alig, T. Villmow, S. Pegel and P. Pötschke, *Polymer*, 2013, **54**, 5865.

22. F. Du, R. C. Scogna, W. Zhou, S. Brand, J. E. Fischer and K. I. Winey, *Macromolecules*, 2004, **37**, 9048.

23. I. Alig, T. Skipa, D. Lellinger and P. Pötschke, *Polymer*, 2008, **49**, 3524.

24. S. Stankovich, D. A. Dikin, R. D. Piner, K. A. Kohlhaas, A. Kleinhammes, Y. Jia, Y. Wu, S. T. Nguyen and R. S. Ruoff, *Carbon*, 2007, **45**, 1558.

25. H. Deng, T. Skipa, R. Zhang, D. Lellinger, E. Bilotti, I. Alig and T. Peijs, *Polymer*, 2009, **50**, 3747.

26. J.-F. Gao, Z.-M. Li, Q.-j. Meng and Q. Yang, *Mater. Lett.*, 2008, **62**, 3530.

27. S. Ochiai, S. Kuboshima, H. Okuda, K. Morishita and E. Tsushima, *Compos. Interface.*, 2014, **21**, 265.

28. A. Kato, Y. Ikeda, R. Tsushi and Y. Kokubo, *J. Appl. Polym. Sci.*, 2013, **130**, 2594.

29. H. H. Le, S. Ilisch and H. J. Radusch, *Polymer*, 2009, **50**, 2294.

30. H. Zou, S. Yan, Y. Sun, L. Zhang and M. Tian, *J. Appl. Polym. Sci.*, 2012, **125**, 3456.

31. H. Deng, L. Lin, M. Ji, S. Zhang, M. Yang and Q. Fu, *Prog. Polym. Sci.*, 2014, **39**, 627.

32. Y. Feng, N. Ning, L. Zhang, M. Tian, H. Zou and J. Mi, *J. chem. phys.*, 2013, **139**, 024903.

33. F. Li, H. Y. Zhang, Y. J. Hu, X. L. Cheng and T. L. Chen, *Advanced Materials Research*, 2011, **152**, 1360.

34. F. Li, Y. Lu, L. Liu, L. Zhang, J. Dai and J. Ma, *Polymer*, 2013, **54**, 2158.

35. S. Araby, Q. Meng, L. Zhang, H. Kang, P. Majewski, Y. Tang and J. Ma, *Polymer*, 2014, **55**, 201.

36. L. Wang, N. Ning, L. Zhang, Y. Lu, M. Tian and T. Chan, *Compos. Part A: Appl. S.*, 2013, **47**, 135.

37. D. Yang, L. Zhang, N. Ning, D. Li, Z. Wang, T. Nishi, K. Ito and M. Tian, *RSC Adv.*, 2013, **3**, 21896.